

Novel Differential Drive Steering System with Energy Saving and Normal Tire Using Spur Gear for an Omni-directional Mobile Robot

Yuki Ueno, Takashi Ohno, Kazuhiko Terashima,
Hideo Kitagawa, Kazuhiro Funato and Kiyooki Kakihara

Abstract—Holonomic omnidirectional mobile robots are useful because of their high level of mobility in narrow or crowded areas, and omnidirectional robots equipped with normal tires are desired for their ability to surmount difference in level as well as their vibration suppression and ride comfort. A caster-drive mechanism using normal tires has been developed to realize a holonomic omnidirectional robot, but some problems has remain. Here we describe effective systems to control the caster-drive wheels of an omnidirectional mobile robot. We propose a Differential-Drive Steering System (DDSS) using differential gearing to improve the operation ratio of motors. The DDSS generates driving and steering torque effectively from two motors. Simulation and experimental results show that the proposed system is effective for holonomic omnidirectional mobile robots.

I. INTRODUCTION

An omnidirectional robot is highly maneuverable in narrow or crowded areas such as including residences, offices, warehouses and hospitals. This technology can be applied to an autonomous mobile robot in a factory, a wheelchair and so on. Several kinds of omnidirectional mobile robots and their applications have been developed [1]-[5]. However, these robots realized their omnidirectional motion by using special wheels such as mecanum wheels, ball wheels, omni-disks and omni-wheels. To improve the ride comfort, vibration suppression, slippage reduction and ability to surmount different in level, omnidirectional robots equipped with normal tires are needed. Arai proposed an omnidirectional vehicle equipped with normal tires [6]. However, it was a non-holonomic vehicle that had to adjust the direction of the wheels before changing the moving direction of the vehicle. Holonomic omnidirectional vehicles, which can move in any direction without changing the direction of the tires beforehand, equipped with normal tires include a dual-wheel type and a caster-drive (active-caster) type [7], [8]. The dual-wheel type has problems as follows. The number of wheels is limited to two, and it is impossible to get high friction or to adapt to a rough terrain by a synchronous drive of many wheels. Moreover, a passive wheel is needed to stabilize the posture of the vehicle.

Y. Ueno, T. Ohno and K. Terashima are with System and Control Laboratory, Production System Engineering, Toyohashi University of Technology, Hibarigaoka, Tempaku, Toyohashi, Aichi, Japan ueno,terasima@syscon.pse.tut.ac.jp

K. Hideo is with the Department of Electrical Control Engineering, Gifu National College of Technology, Kamimakuwa, Motosu, Gifu, Japan hkita@gifu-nct.ac.jp

K. Funato and K. Kakihara are with the KER CO., LTD, Yutakagaoka, Toyokawa, Aichi, Japan kfunato,kkakihara@ker-jp.com

The caster-drive wheel has an offset between the steering axis and the center of the wheel. The wheel can move in any direction by controlling the steering axis and the driving wheel independently by using two motors. Holonomic omnidirectional motion of a robot can be realized by using two or more caster-drive wheels. However, the caster-drive wheel also has a problem as follows. When the vehicle is in steady motion, including straight motion and rotation with constant curvature, only the driving motor works and the steering motor becomes idle. When the vehicle changes its moving direction, high load is applied to the steering motor. Therefore, high power is required both for the driving and steering motors, which means the vehicle's mass is increased.

The aim of our research is therefore to develop a holonomic omnidirectional mobile robot with a caster-drive wheel minimizing the motor power by using the interference of the output of two motors. A new gearing mechanism is proposed to realize the interference. Furthermore, the proposed method is shown to be effective, because it is possible to surmount difference in level and it absorbs the vibration by using normal tires.

II. PRINCIPLE

A. Omnidirectional Motion Using a Caster-Drive Wheel

Fig. 1 shows the caster-drive wheel. Two degrees of freedom can be generated in the steering axis using this mechanism. Longitudinal force is generated by the wheel rotation. Lateral force is generated with the rotation of the steering axis because of the friction between the floor and wheel. The position and orientation of the wheel can be represented by the position $O_w(X_w, Y_w)$ of the steering axis and the orientation θ_w as shown in Fig. 1.

By rotating the driving wheel with the angular velocity ω_w , velocity $\dot{x}_w = r\omega_w$ is generated in the direction of the X_w axis. Here, r is the radius of the driving wheel. By rotating the steering axis with the angular velocity ω_l , velocity $\dot{y}_w = -l\omega_l$ would be generated at the center of the wheel in the direction of the Y_w axis. Here, l is the offset distance between the steering axis and the center of the driving wheel in the direction of X_w . However, reacting velocity $\dot{y}_w = l\omega_l$ is generated at the steering axis in the direction of the Y_w axis, because the position of the driving wheel is fixed by the friction with the ground. Therefore, the velocity (\dot{x}_w, \dot{y}_w) of the caster-drive wheel can be controlled by changing ω_w and ω_l .

Fig. 2 shows an example of motion. The initial orientation θ_w of the wheel is set to be $\theta_w = \pi/2$ rad in the frame

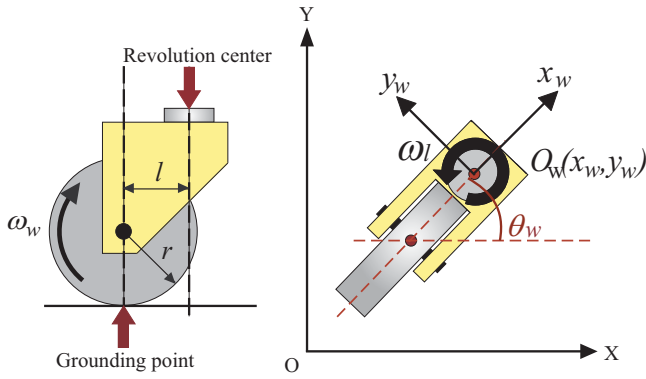


Fig. 1. Model of the caster-drive wheel

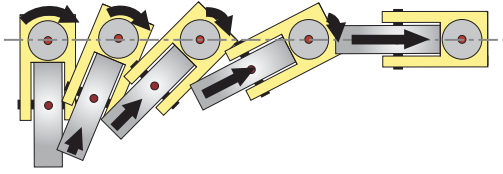


Fig. 2. Lateral motion to right.

$O - XY$. The motion, as shown in Fig. 2, can be given by changing ω_w and ω_l appropriately. Even though the rotating wheel itself cannot generate lateral motion to the right, the lateral motion of the robot, which is fixed to the steering axis, is realized. No wheel has to control the orientation of the robot by itself. The direct kinematic equation is denoted by the state vector $x_w = [x_w, y_w]^T$ and the input vector $u_w = [\omega_w, \omega_l]^T$ as

$$\dot{x}_w = B_w u_w \quad (1)$$

where

$$B_w = \begin{bmatrix} r \cos \theta_w & -l \sin \theta_w \\ r \sin \theta_w & l \cos \theta_w \end{bmatrix} \quad (2)$$

The inverse kinematic equation becomes

$$u_w = B_w^{-1} \dot{x}_w \quad (3)$$

where

$$B_w^{-1} = \begin{bmatrix} \frac{1}{r} \cos \theta_w & \frac{1}{l} \sin \theta_w \\ -\frac{1}{r} \sin \theta_w & \frac{1}{l} \cos \theta_w \end{bmatrix} \quad (4)$$

Holonomic omnidirectional motion $(\dot{x}, \dot{y}, \dot{\theta})$ of a mobile robot can be achieved by using two or more caster-drive wheels.

B. Differential-Drive Steering System (DDSS)

We developed a useful method for constructing a caster-drive wheel using a Differential-Drive Steering System (DDSS). The DDSS outputs driving and steering velocities from two motors using differential gearing. Fig. 3 shows the principle of the DDSS. The differential gearing mechanism is realized by using five spur gears, referred to as A, B, C, C' and D. A is engaged with C', and B is engaged with C through the counter gear. C and C' are fixed to each other. The DDSS is a 2-input/2-output system without fixing any component.

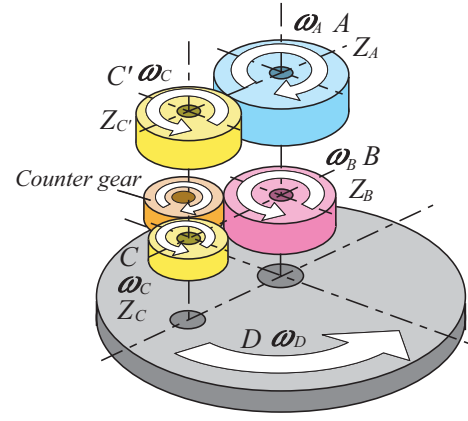


Fig. 3. Principle of the proposed DDSS

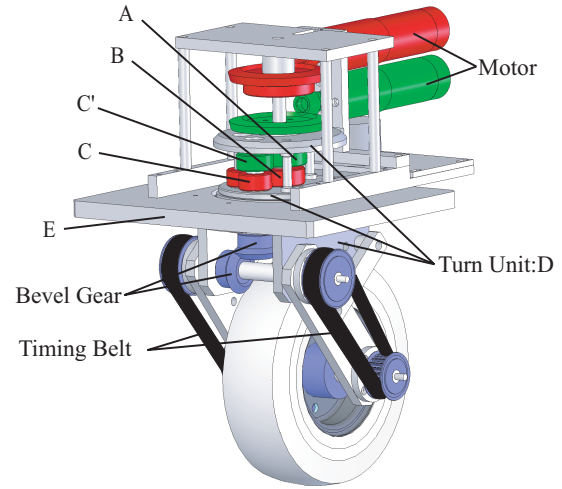


Fig. 4. Mechanism of the proposed DDSS

A and B are independently driven by two motors. C and D provide output torque. Fig. 4 shows the mechanism of the DDSS. Torques of two motors are transmitted to the DDSS by a bevel gear, D, which is fixed to the chassis E, provides the steering torque, and C, which leads to the driving wheel via the bevel gear, provides the driving torque. Let $\omega_A, \omega_B, \omega_C, \omega_C'$ and ω_D be of the angular velocity of A, B, C, C' and D in Fig. 3, and Z_A, Z_B, Z_C and Z_C' be the number of teeth of A, B, C and C', respectively. When $\omega_D = 0$, the steering angular velocity ω_l becomes zero, and we obtain

$$\omega_A = \frac{Z_C}{Z_A} \frac{Z_B}{Z_C} \omega_B = \frac{Z_C}{Z_A} \omega_C \quad (5)$$

$$\omega_D = 0 \quad (6)$$

When $\omega_C - \omega_D = 0$, the driving angular velocity ω_w becomes zero because C does not rotate between A and B, and we obtain

$$-\omega_A = \omega_B = \omega_C (= \omega_C') = \omega_D \quad (7)$$

The direct kinematic equation, which derives driving and steering output $u_w = [\omega_w, \omega_l]^T$ from motor input $u_P = [\omega_A, \omega_B]^T$, can be described as

$$u_w = \begin{bmatrix} \omega_C - \omega_D \\ \omega_D \end{bmatrix} = B_P u_P \quad (8)$$

where

$$B_P = \begin{bmatrix} \frac{Z_A Z_B}{Z_A Z_C + Z_B Z_C} & \frac{Z_A Z_B}{Z_A Z_C + Z_B Z_C} \\ -\frac{Z_A Z_C}{Z_A Z_C + Z_B Z_C} & \frac{Z_B Z_C}{Z_A Z_C + Z_B Z_C} \end{bmatrix} \quad (9)$$

The inverse kinematic equation becomes

$$u_P = B_P^{-1} u_w \quad (10)$$

where

$$B_P^{-1} = \begin{bmatrix} \frac{Z_C}{Z_A} & -1 \\ \frac{Z_C}{Z_B} & 1 \end{bmatrix} \quad (11)$$

Next, we derive the motor power ratio of the DDSS. Joint torques T_A, T_B, T_C and T_D of A, B, C and D, respectively, are given by

$$\begin{bmatrix} T_C \\ T_D \end{bmatrix} = \begin{bmatrix} \frac{Z_B}{Z_C} & \frac{Z_A}{Z_C} \\ -\frac{Z_B}{Z_C} & \frac{Z_A}{Z_C} \end{bmatrix} \begin{bmatrix} T_A \\ T_B \end{bmatrix} \quad (12)$$

where the positive direction of each torque is same as that of angular velocity in Fig. 3.

For an omnidirectional mobile robot with the DDSS, steady motion including straight motion and rotation with constant curvature is achieved by $\omega_l (= \omega_D) = 0$. When $\omega_l = 0 (T_D = 0)$, the joint torques are given from (12) by

$$T_A = \frac{Z_C}{Z_B} \frac{Z_A}{Z_C} T_B \quad (13)$$

$$T_C = -\frac{2Z_B}{Z_C} T_A \quad (14)$$

$$T_D = 0 \quad (15)$$

The power ratio of two motors is given from (5) and (13) by

$$\begin{aligned} P_A : P_B &= T_A \omega_A : T_B \omega_B \\ &= \left(\frac{Z_C}{Z_B} \frac{Z_A}{Z_C} T_B \right) \left(\frac{Z_C}{Z_A} \omega_C \right) : T_B \frac{Z_C}{Z_B} \omega_C \\ &= 1 : 1 \end{aligned} \quad (16)$$

On the other hand, when $\omega_w = 0 (T_C = 0)$, the joint torques are given from (12) by

$$T_A = -\frac{Z_C}{Z_B} \frac{Z_A}{Z_C} T_B \quad (17)$$

$$T_C = 0 \quad (18)$$

$$T_D = \frac{2(Z_B)}{Z_C} T_A \quad (19)$$

The power ratio is given from (7) and (17) by

$$\begin{aligned} P_A : P_B &= T_A \omega_A : T_B \omega_B \\ &= \frac{Z_C}{Z_B} \frac{Z_A}{Z_C} T_B \omega_B : T_B \omega_B \\ &= \frac{Z_C}{Z_B} : \frac{Z_C}{Z_A} \end{aligned} \quad (20)$$

When $\frac{Z_C}{Z_B}$ is equal to $\frac{Z_C}{Z_A}$, the power ratio yields

$$P_A : P_B = 1 : 1 \quad (21)$$

III. OPERATION RATIO OF MOTORS

To examine the operation ratio of motors, we compare the DDSS to a conventional caster-drive wheel. We define the operation ratio δ of motors as

$$\delta = \frac{(\text{Sum of motor power in motion})}{(\text{Sum of rated power of motors})} \quad (22)$$

The ratio ($P_{A0} : P_{B0}$) of the rated power of two motors used in the DDSS is set to be 1:1. The ratio of rated power used in the conventional method is also set to be 1:1, as denoted in Wada [8].

We calculate the operation ratio δ in the case of driving motion ($T_D = 0$). Let P be the sum of motor output power needed to achieve the motion. The result of the conventional method is $P_{A0} = P_{B0} = P$ and $\delta = \frac{P}{P_{A0} + P_{B0}} = 0.5$. The result of the DDSS is $P_{A0} = P_{B0} = \frac{P}{2}$ and $\delta = \frac{P}{P_{A0} + P_{B0}} = 1$.

Next, we calculate δ in the case of steering motion ($T_C = 0$). The result of the conventional method is $P_{A0} = P_{B0} = P$ and $\delta = 0.5$. The result of the DDSS is $P_{A0} = P_{B0} = \frac{P}{2}$ and $\delta = \frac{P}{P_{A0} + P_{B0}} = 1$.

The output power of motors can be decreased by using the DDSS as a caster-drive wheel because of its high operation ratio of motors. This means that the size of the robot can be smaller by using the DDSS.

IV. CONSTRUCTION OF OMNIDIRECTIONAL MOBILE ROBOT

We constructed a prototype model of a vehicle with four DDSS wheels to check the feasibility of the proposed mechanism, as shown in Fig. 5. Effectiveness of the proposed DDSS was confirmed by this apparatus. Fig. 6 and Table I show a figure and the specifications of a platform of the omnidirectional mobile robot with four DDSS wheels, respectively. The proposed omnidirectional robot has the capability of climbing a slope of 12 deg and exceeding a difference of 70 mm while carrying a load of 100 kg. Offset distance, l , can be adjusted in this unit by trial and error. If the offset distance is larger, the straight run



Fig. 5. Photograph of the four-wheeled vehicle built in the authors laboratory

TABLE I
SPECIFICATION OF THE VEHICLE

Size (D × W × H)	800 × 700 × 1280 (mm)
Weight	80 (kg)
Motor power	150 (W) × 8
Max. velocity	6 (km/h)
Max. acceleration	2.0 (m/s ²)
Max. slope angle	12 (deg)
Max. step difference	70 (mm)
Max. loading weight	100(kg)
Diameter of wheel	210 (mm)
Offset distance	8 - 56 (mm)

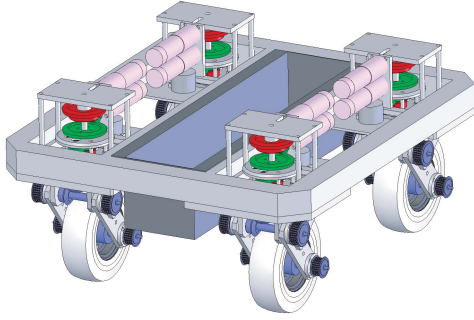


Fig. 6. Platform of the proposed omnidirectional mobile robot

becomes stable and the demand value of angular velocity of the steering becomes smaller. In this case, larger torque is needed in the steering axis. On the other hand, when the offset distance is smaller, the straight run is unstable, but the mobility is improving. In addition, the torque in the steering axis is smaller, while the angular velocity of the steering axis becomes larger. There is a contrastive relationship between torques, angular velocity and stability of the wheel. Therefore, it is necessary to think about the offset distance from the experiment. From that reasons, the offset distance can be adjusted between 8 mm and 56 mm in consideration of the motor capacity. In this paper, offset distance is tentatively given as 25 mm.

A. Kinematic Model of a Four-wheeled Vehicle

A caster-drive wheel generates two degrees of freedom on the demensional plane. To generate omnidirectional movement on the ideal flat floor, a vehicle must have at least two wheels to control three degrees of freedom in total, which includes two translation degrees of freedom and an attitude degree of freedom. However, a real road surface contains a nonideal floor. In consideration of vehicle stability on the nonideal floor, we adopted a control system for a four-wheeled vehicle.

Fig. 7 shows a schematic model of the four-wheeled vehicle. The kinematic model is described follows:

$$\begin{bmatrix} \dot{x}_v \\ \dot{y}_v \\ \dot{\theta}_v \end{bmatrix} = \begin{bmatrix} \frac{1}{4} & 0 & -\frac{1}{4}(x_{va} \sin \theta_v + y_{va} \cos \theta_v) \\ 0 & \frac{1}{4} & \frac{1}{4}(x_{va} \cos \theta_v - y_{va} \sin \theta_v) \\ \frac{1}{4} & 0 & -\frac{1}{4}(x_{vb} \sin \theta_v + y_{vb} \cos \theta_v) \\ 0 & \frac{1}{4} & \frac{1}{4}(x_{vb} \cos \theta_v - y_{vb} \sin \theta_v) \\ \frac{1}{4} & 0 & -\frac{1}{4}(x_{vc} \sin \theta_v + y_{vc} \cos \theta_v) \\ 0 & \frac{1}{4} & \frac{1}{4}(x_{vc} \cos \theta_v - y_{vc} \sin \theta_v) \\ \frac{1}{4} & 0 & -\frac{1}{4}(x_{vd} \sin \theta_v + y_{vd} \cos \theta_v) \\ 0 & \frac{1}{4} & \frac{1}{4}(x_{vd} \cos \theta_v - y_{vd} \sin \theta_v) \end{bmatrix}^T \begin{bmatrix} \dot{x}_a \\ \dot{y}_a \\ \dot{x}_b \\ \dot{y}_b \\ \dot{x}_c \\ \dot{y}_c \\ \dot{x}_d \\ \dot{y}_d \end{bmatrix} \quad (23)$$

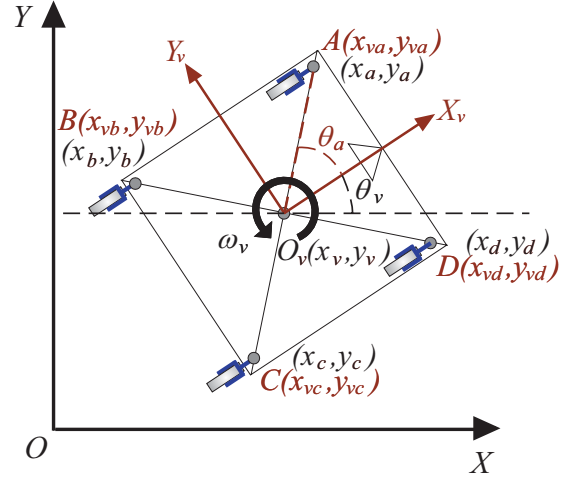


Fig. 7. Model of the vehicle

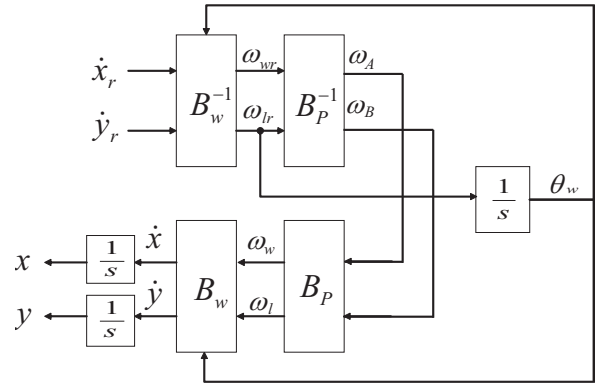


Fig. 8. Block diagram of the single wheel

Then, the inverse kinematic model is described as follows:

$$\begin{bmatrix} \dot{x}_a \\ \dot{y}_a \\ \dot{x}_b \\ \dot{y}_b \\ \dot{x}_c \\ \dot{y}_c \\ \dot{x}_d \\ \dot{y}_d \end{bmatrix} = \begin{bmatrix} 1 & 0 & -y_{va} \cos \theta_v - x_{va} \sin \theta_v \\ 0 & 1 & x_{va} \cos \theta_v - y_{va} \sin \theta_v \\ 1 & 0 & -y_{vb} \cos \theta_v - x_{vb} \sin \theta_v \\ 0 & 1 & x_{vb} \cos \theta_v - y_{vb} \sin \theta_v \\ 1 & 0 & -y_{vc} \cos \theta_v - x_{vc} \sin \theta_v \\ 0 & 1 & x_{vc} \cos \theta_v - y_{vc} \sin \theta_v \\ 1 & 0 & -y_{vd} \cos \theta_v - x_{vd} \sin \theta_v \\ 0 & 1 & x_{vd} \cos \theta_v - y_{vd} \sin \theta_v \end{bmatrix} \begin{bmatrix} \dot{x}_v \\ \dot{y}_v \\ \dot{\theta}_v \end{bmatrix} \quad (24)$$

Therefore, when \dot{x}_v , \dot{y}_v and $\dot{\theta}_v (= \omega_v)$ are given, the velocity ($\dot{x}_a, \dot{y}_a, \dot{x}_b, \dot{y}_b, \dot{x}_c, \dot{y}_c, \dot{x}_d, \dot{y}_d$) of four wheels is calculated by using (24), where \dot{x}_v, \dot{y}_v and ω_v indicate the velocity in the X-direction, Y-direction and the angular velocity of the vehicle, and $x_{va}, y_{va}, x_{vb}, y_{vb}, x_{vc}, y_{vc}, x_{vd}$ and y_{vd} indicate the coordinate of each wheels on the local coordinate system, respectively.

V. SIMULATION AND EXPERIMENT

A. Simulation of the Single Wheel

To check the kinematic model of the DDSS, we simulated the motion of the wheel. Fig. 8 shows a block diagram of the control system. If ordered velocity \dot{x}_r and \dot{y}_r were given, the angular velocities of gears ω_A and ω_B are calculated

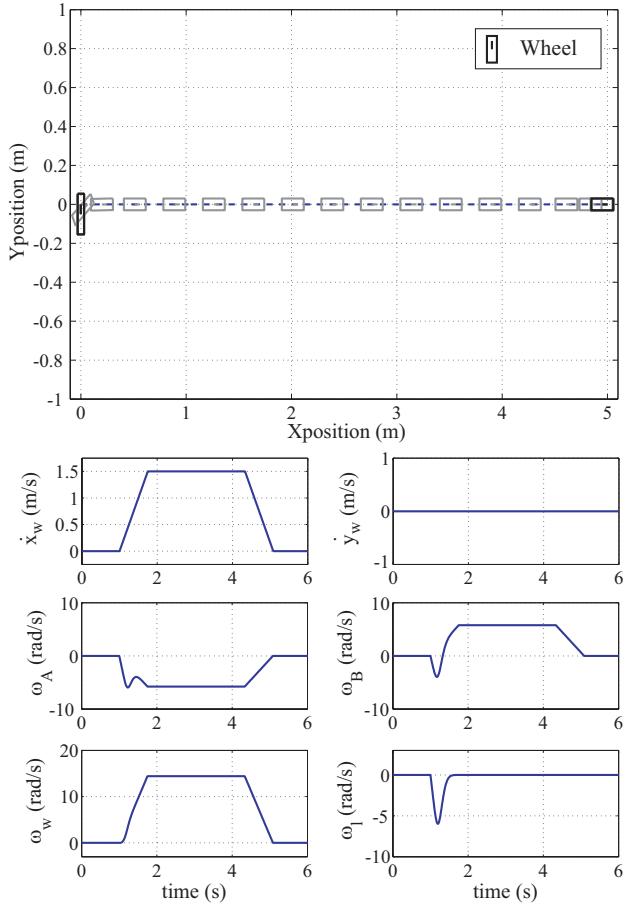


Fig. 9. Simulation results of the single wheel

by using (11). θ_w is the steering angle of the wheel which is the integral calculus value of steering angular velocity ω_l . However, in fact, the wheel angle is detected from the absolute encoder attached to the steering axis.

Translational motion toward the +X direction with a maximum velocity of 6 km/h (=1.67 m/s) and a maximum acceleration of 0.5 m/s² was examined. The initial value of θ_w was set as 1.57 rad (=90 deg) in this case.

Fig. 9 shows the simulation result, where, \dot{x}_w , \dot{y}_w , ω_A , ω_B , ω_w and ω_l indicate the velocity in the X-direction, Y-direction, the angular velocity of gear A and the gear B, the angular velocity of the wheel and the steering axis, respectively. As shown from the simulation result, the wheel can move to reference directions instantly and independently of the initial angle of the wheel. In addition, graphs of the angular velocity of two motors, ω_A and ω_B , show that the DDSS can be generated driving and steering torques by using two motors simultaneously as indicated by ω_l and ω_w .

B. Simulation and Experiment with the Four-wheeled Vehicle

To verify the mobility of the vehicle, we examined its X-axis direction translation movement. Initially the wheels are pointed in different directions, and the value of θ_v was set to be 1.57 rad in this case.

Fig. 10 shows the simulation result of the four-wheeled vehicle. The rectangle, triangle and four smaller rectangles in the graph indicates the vehicle body, front of the vehicle

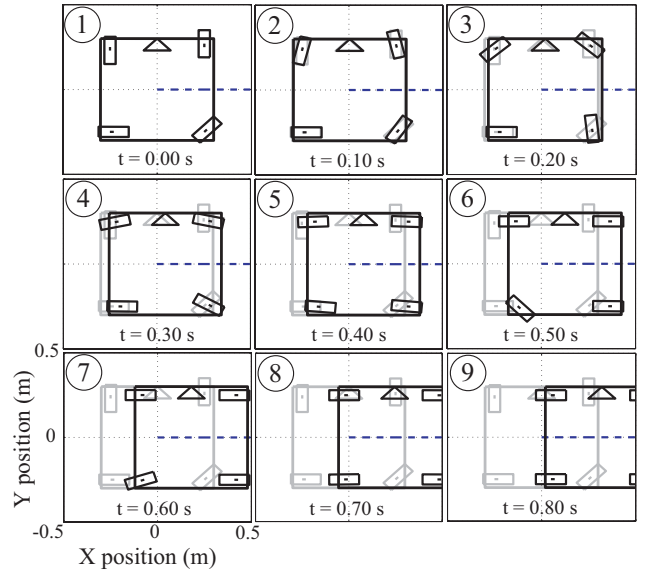


Fig. 10. Simulation result of the vehicle

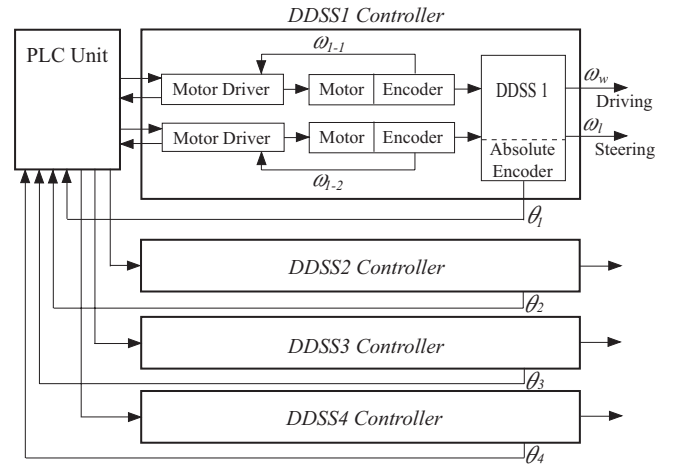


Fig. 11. Control system of the vehicle

and wheels, respectively. From the results, the vehicle can move to goal direction instantly, despite the difference in the ways the wheels point, by solving inverse kinematics of (24) and (3).

Fig. 11 is a block diagram of the control system of the vehicle. A programmable logic controller (PLC) unit is used for controlling the vehicle. The PLC unit has various exclusive units such as the CPU unit, logic input and output unit and analog input and output unit.

Each wheel angle is detected from an absolute encoder attached to the steering axis by using the input unit. To control DC motors, an exclusive motor driver is used. The rotation speed of DC motors is controlled by the motor driver, and reference for the revolution speed is given by analog voltage from the analog output unit. The CPU unit is used for resolving the kinematic equation from the angle of each wheel and reference velocities and obtaining each motor's angular velocity. The calculated angular velocity is transformed to analog voltage and transmitted to the motor driver, and the vehicle is controlled. When experiments are

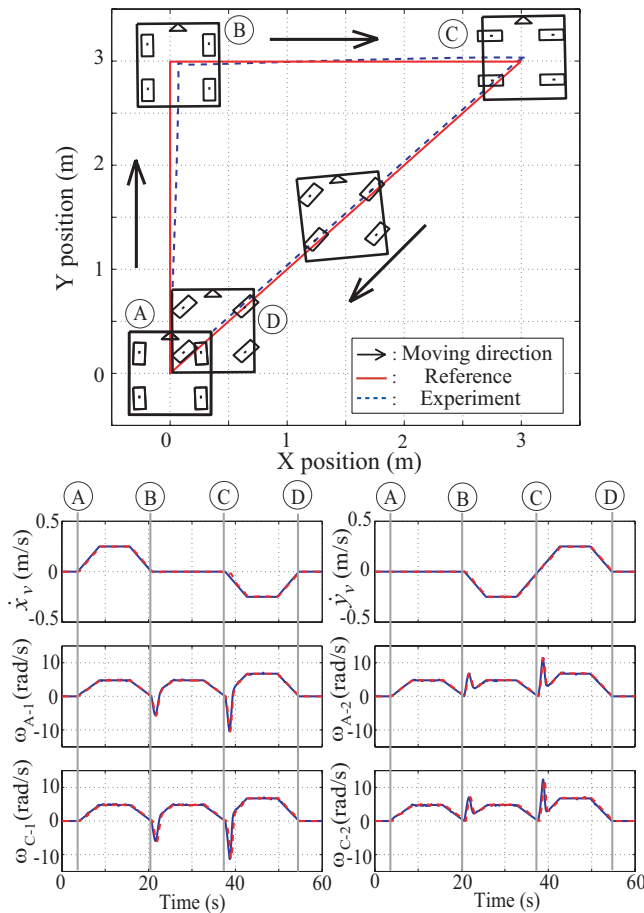


Fig. 12. Experimental result of the vehicle

performed, the x-y position of the vehicle can be computed from the encoder signal.

Fig. 12 shows the experimental result of the four-wheeled vehicle. In addition, \dot{x}_v , \dot{y}_v , ω_{A-1} , ω_{A-2} , ω_{C-1} , ω_{C-2} indicates the velocity in the X-direction, Y-direction, the angular velocity of motors in wheel-A (motor:A-1 and A-2) and the angular velocity of motors in wheel-C (motor:C-1 and C-2), respectively. We examined autonomous moving by using a velocity pattern that was generated beforehand. The pattern of motion was at the first translation movement forward, the second translation movement rightward and finally the translation movement to 45 degrees in the left rear side.

From the result, we see that there is a little error trajectory with respect to the reference. It is considered to be the result of the large amount of friction between the tire and the floor because the error trajectory is generated when the move direction changes. We should be able to avoid this problem in future by adding a feedback control system. On the other hand, when the control system of a vehicle consists of a manual control system such as a joystick or power assist system, the vehicle does not require strict trajectory control, because the operator is doing fine adjustment of the vehicle themselves. The error of the angle of the vehicle in the translation movement affects its operability, so we need to improve stability of the straight-run in the future.

VI. CONCLUSIONS AND FUTURE WORKS

A. Conclusions

In this paper, a novel Differential-Drive Steering System (DDSS) is proposed for the caster-drive wheel of a holonomic omnidirectional mobile robot, and omnidirectional mobile robot based on the proposed mechanism is newly built. The DDSS can provide a high operation ratio of motors compared to a conventional caster-drive wheel. Numerical analysis and experiments by building a prototype novel vehicle showed the effectiveness of the DDSS.

B. Future Works

Future works include the following:

- Posture control on rough terrain.
- Evaluation of vibration test on the ground.
- Application to an omnidirectional wheelchair.

VII. ACKNOWLEDGMENTS

We would like to express my gratitude to Prof. Miyoshi and Dr. Yoshiyuki Noda for their advice to develop this research.

This work was supported by the 21st Century COE Program "Intelligent Human Sensing", and also G-COE "Frontier of Intelligent Sensing", and furthermore by Aichi Science & Technology Foundation Research Aid Project of 2008 and 2009 year. We would like to address the sincere thanks.

REFERENCES

- [1] M. West and H. Asada, "Design of a holonomic omnidirectional vehicle," Proc. IEEE Int. Conf. Robot. Automat., 1992, pp.97-103.
- [2] F. G. Pin and S. M. Killough, "A new family of omni-directional and holonomic wheeled platforms for mobile robots," IEEE Trans. Robot. Automat., 1994, vol.10, pp.480-489.
- [3] R. Damoto and S. Hirose, "Development of Holonomic Omnidirectional Vehicle "Vuton-II" with Omni-Discs," Journal of Robotics and Mechatronics, 2002, Vol.14, No.2, pp.186-192.
- [4] K. Terashima, H. Kitagawa, T. Miyoshi and J. Urbano, "Frequency Shape Control of Omni-directional Wheelchair to Increase User's Comfort," Proc. IEEE 2004 Int. Conf. on Robotics and Automation, New Orleans, 2004, pp.3119-3124
- [5] J. Urbano, K. Terashima, "Skill-Assist Control of an Omni-directional Wheelchair by Neuro-Fuzzy Systems Using Attendant's Force Input," International Journal of IJICIC(International Journal of Innovative Computing, Information & Control), Vol.2, No.6, Dec., 2006, pp.1219-1248.
- [6] T. Arai, E. Nakano, H. Hashino and K. Yamaba, "The Control and Application of Omni-Directional Vehicle (ODV)," Proc. 8th IFAC World Congress, 1981, pp.1855-1860.
- [7] M. Wada, A. Takagi and S. Mori, "A Mobile Platform with a Dual-wheel Caster-drive Mechanism for Holonomic and Omnidirectional Mobile Robots," Journal of Robotics Society of Japan, 2000, Vol.18, No.8, pp.1166-1172.
- [8] M. Wada and S. Mori, "Holonomic and omnidirectional vehicle with conventional tires," Proc. IEEE Int. Conf. on Robotics and Automation, 1996, pp.3671-3676.
- [9] K. Tadakuma, R. Tadakuma and J. Berengeres, "Development of Holonomic Omnidirectional Vehicle with "Omni-Ball": " Spherical Wheels," Proc. IEEE/RSJ International Conference on Intelligent Robots and Systems, 2007, pp.33-39.
- [10] S. Kim, H. Kim and B. Moon, "Local and Global Isotropy of Caster Wheeled Omnidirectional Mobile Robot," Proc. IEEE International Conference on Robotics and Automation, 2005, pp.3446-3451.